Seismic performance assessment of intermediate moment-resisting steel frames designed based on misidentified site soil classes

Vahid Broujerdian*, Esmaeil Mohammadi Dehcheshmeh, Pouria Safari

* Corresponding author: Vahid Broujerdian
Postal address: School of Civil Engineering, Iran University of Science & Technology, P.O. Box 16765-163, Narmak, Tehran, Iran. Tel.: +98 21 77240399. Fax: +98 2177240398. E-mail address: broujerdian@iust.ac.ir

School of Civil Engineering, Iran University of Science and Technology, Tehran, Iran

Abstract:
This research aims to investigate the extent that an incorrect assumption for soil type may endanger the seismic safety of moment-resisting steel frame structures using probabilistic assessment. To this aim, first, a set of moment-resisting steel frame structures were designed for the site soil class C. The examined structures were 3-, 6-, and 9-storey designed by CSI ETABS software according to ASCE7-16. Then, assuming that the actual soil type had been B, C, or D, seismic vulnerability assessments were performed using OpenSees software. For this purpose, a two-dimensional model of each structure was undergone the incremental nonlinear dynamic analysis (IDA) subjected to far-field, near-field (with pulse), and near-field (without pulse) ground motions of FEMA-P695. The fragility curves were developed for each model under each ground motion record type and accordingly the collapse margin ratio for each model was calculated. The results indicated that within the LS performance level at $S_{a(Design)}$, site soil class B decreases the exceedance probability slightly but site soil class D tends to increase the exceedance probability significantly, especially as the height increases. Furthermore, it was found that the soil-structure interaction (SSI) has a negligible effect on the collapse margin ratio in all the investigated models.

Keywords: Site Soil Class, Soil-Structure Interaction, Moment-Resisting Steel Frames, Fragility Curves, Exceedance Probability.

1. Introduction

Accomplishing a standard geotechnical investigation leads to saving construction costs and it will lower its associated risks such as construction failures, time overruns, and delays [1]. The process of subsurface soil classification and stratification (or zonation) is highly important for preparing the geotechnical site report before tending to commence any design and construction of structures [1-7]. However, considering various limitations such as shortage of time, lack of budget, not having suitable access to subsurface soil, and more practically, insufficient information collected from site investigation spots in terms of the number of boreholes and cone penetration tests (CPTs) [8-14], this process may lead to challenging sessions of interpreting the gathered data and considerable uncertainties in classified soil samples [4, 11, 13, 14]. It has been investigated that the quality of the data obtained from site investigations can greatly affect the risk of foundation failure which can be reduced by increasing the scope of the site investigation [15]. A conducted study in the UK has shown that uncertainties in site soil classification results in nearly 22% of geotechnical deficits [16]. Recent studies conducted on the quality of the site investigation samples have achieved promising results; a data-driven study conducted on the efficiency of the sampling locations and several site investigations proposed an effective method using the Voronoi diagram and Bayesian compressive sampling [17]. Optimal site investigations through the use of random, virtual soils in a Monte Carlo analysis context indicated that can lower the risk of damage associated with inaccurate site investigations and save great values of the budget during and after construction [18, 19]. An effective method for characterization of the subsurface stratigraphic configuration with limited borehole data was proposed which captures the spatial correlation between different subsurface zones using an autocorrelation function [20].

So, it is inevitable not to fully rely on geotechnical site investigation and it would be useful for increasing the structural safety to consider soil failure scenarios at the time of engineering design of structures.

Different procedures are introduced for the assessment of seismic demand. Comparatively, The Incremental nonlinear Dynamic Analysis method (IDA) is a procedure with the most precise performance [21]. In the method of IDA, the structure is evaluated against a broad range of ground motion records resulting in the extraction of uniformed IDA curves, and subsequently, by plotting the corresponding fragility curves, collapse probability can be calculated [22].

Previously accomplished investigations emphasize the essential role of flexible foundations in the structural design of buildings [23]. These researches showed that consideration of SSI in site soil class of C adapts to lower exceedance probability and the soil shear modulus was identified to be much affecting the fragility curves [24, 25]. The substantive role of liquefaction and SSI in altering the seismic fragility and vulnerability of non-ductile low-rise RC frame buildings was investigated and it was shown that soil behavior during strong shaking significantly affects the vulnerability of the soil-foundation-structure system [26-28]. In another research, the effects of soil deformability and structural flexibility on the non-linear response of the system were assessed [29]. It was indicated that the nonlinear soil behavior leads mostly to an increase in seismic collapse probability compared to linear soil behavior and fixed-base conditions [30]. Investigating the effect of different SSI models on the seismic fragility functions, it was revealed that the inelastic behavior leads to more energy dissipation and smaller displacements [31]. Considering all three components of near-field ground motions and elimination of the foundation rocking's inter-storey drift proved to increase the accuracy of the seismic structural responses [32]. And, the necessity of considering flexible foundations in the seismic design of low-rising structures was positively emphasized to be a contributing factor for increasing the accuracy of responses through the application of performance levels [33].

In general, the effect of various site soil classes on the collapse assessment of steel structures needs to be assessed to determine the influence of each soil class on the collapse probability in a comparative-based framework.

This research aims to investigate the effect of various site soil classes on the exceedance probability of intermediate moment-resisting steel frame structures considering SSI in a scenario in which the geotechnical investigation has reported a false site soil class. It means, it is assumed that the initial models are designed for a specific type of soil but after the construction, it is revealed that the reported site soil class is not accurately chosen. So, for assessing the exceedance probability of the designed structure, it would be essential to investigate its fragility considering the real site soil class. For this purpose, three models of 3-, 6-, and 9-story frame structures with intermediate moment-resisting frame systems are designed according to ASCE7-16 using the CSI ETABS software considering a site soil class C. In the next stage, 2D frames of the investigated models are simulated in fixed-base and flexible-base conditions. The "Beam on Nonlinear Winkler Foundation" (BNWF) method was chosen for SSI modeling. To account for the false report of the geotechnical investigation, 2D frames that were initially chosen from investigated models designed for site soil class C are also analyzed with two other classes B and

D. Through a procedure by OpenSees software, selected 2D models with fixed and flexible foundations designed for the site soil class C are analyzed using IDA method subjected to far-field, near-field (with pulse) and near-field (without pulse) ground motion records of FEMA-P695, and it was mentioned for investigating the effect of false site soil class on exceedance probability of the models, two other soil classes B and D are used in the SSI specification of the initially designed models. At this stage, fragility curves are developed for each model under each ground motion record type and the collapse margin ratio for each model is also calculated. By accomplishing these stages, at the final step, the exceedance probability of investigated models is compared and the effect of SSI with various site soil classes is assessed, also the acquired collapse margin ratio will draw a safety assessment for understanding the effect of SSI when the geotechnical report is reported falsely.

2. Methodology

2.1. Site Soil Classification

ASCE7-16 [34] states that the site soil shall be classified as A, B, C, D, E, and F based on the upper 30 m of the site profile. Where the site-specific data are not available to a depth of 30 m, appropriate soil properties are permitted to be estimated by the registered design professional preparing the soil investigation report based on known geologic conditions. In addition, where the soil properties are not known in sufficient detail to determine the site class, site class D shall be used unless the authority having jurisdiction or geotechnical data determining site class E or F soils are present at the site. In this study, the investigated models are designed for site soil class C but at the next stage, a scenario is drawn in which it is supposed that the geotechnical report turns out to be inaccurate. So, to assess the exceedance probability of the already designed structures for site soil class C, two other soil classes B and D are chosen to be used in the SSI simulation in the collapse assessment of the structures. The reason for designing the models for site soil class C and considering sits soil classes B and D for the inaccurate geotechnical report are due to their prevalence and rather more distribution in various soil profiles in seismic regions [35] compared with site soil classes A, E and F. Table 1 shows the considered site soil classes according to the classification of ASCE7-16 [34].

2.2. Specifications of the Models

In this study, three models of 3-, 6-, and 9-storey were designed by CSI ETABS 2016 [36] according to the method of LRFD and based on ASCE7-16 consideration [34] with modification factor 4.5 (R=4.5) and impotence factor 1 (I=1). Designed models are the same as the ones used previously in another research paper of the authors [23]. The models were designed for a region with very high level of seismic intensity (Risk Category II and Seismic Design Category D) with parameters S_s=1.5 and S_1=0.6. Associated risk and seismic category of the structures respectively is II and D. Investigated models are regular both in plan and height with the area of 375m^2 (15m × 25m) consisted of 3 spans of 5m in X direction, 5 spans of 5m in Y direction and height of each floor is considered equal to 3.2m, and it has to be mentioned that in the process of calculating the required structural demands of each member, demand-capacity ratio (DCR) of beams and columns was respectively limited to 0.7-1.0 and 0.6-0.9 so that more than 85% of structural members' DCRs stay within this interval. Mechanical properties of the used steel are considered to be 2.0E5 MPa for modulus of elasticity, 240 MPa for yield stress, 370 MPa for

ultimate stress and 0.25 as the ultimate strain, and for concrete, modulus of elasticity and compressive strength considered to be equal to 2.0E4 MPa and 25 MPa. Designed cross-sections (European steel profiles) and geometrical dimensions of the foundation of each model are indicated in Table 2. Also, during the design procedure, at the bottom of columns in ground zero elevation, the restraining condition is considered as rigid connections, and after extracting detailed forces of the structure, footings of the models were designed separately as strip foundations. Figure 1 presents the structural plan and 3D view of the investigated models [23].

2.3. Incremental Dynamic Analysis (IDA)

IDA as an advanced method for nonlinear dynamic analysis presents the result of seismic capacity versus demand of structures (IDA Curves) by applying ground motion records till the collapse point. Subsequently, by plotting the graphs of intensity level versus response and applying limit states, the assessment of the structure can be accomplished. Using this type of analysis enables the engineers to assess the structural behaviour of the models from linear elastic to nonlinear inelastic phase through a step-by-step process which results in a precise approximation of the seismic safety of the investigating structural models [23].

It is stated by PEER [37] that the parameter of intensity measure (IM) be selected from seismic risk analysis to be applied to the structure. An Engineering Demand Parameter (EDP) results from the corresponding structural response to each IM or Damage Measure (DM), furthermore, by introducing a damage index the exceedance probability from will be specified and used for estimating the rehabilitation costs [37].

In this study like the previous research paper of the authors [23], the spectral acceleration of records corresponding to the first mode of the structure with a damping ratio of 5%; i.e., Sa (T1, 5%) is used as IM. This parameter is more efficient for extracting the IDA curves than other quantities like PGA because it has far less data scattering. Furthermore, the maximum inter-story drift ratio is chosen as DM for IDA curves.

2.4. FEMA-P695 Ground Motion Records

Since it is the objective of the present paper to study the effect of various site soil classes on the seismic safety of the models under various ground motion records, therefore, three sets of ground motion records consisting of 22 far-field, 14 near-field (with pulse), and 14 near-field (without pulse) from the FEMA-P695 manual [24] are used as shown in Tables 3 to 5.

2.5. Numerical Simulation

Thorough description of the numerical simulation of the investigated models of this study by the OpenSees software [38] is available in the authors' previous research paper [23]. Structural geometries, boundary conditions and material properties were set based on the designed models. For simulating the models by OpenSees, the "Fibre" section was selected for the profiles, and "NonLinear Beam-Column" as the appropriate structural element [23]. SSI consideration is fully discussed in the previous research paper [23] too. Comparatively, the method of "Beam on Nonlinear Winkler Foundation" (BNFW) as recommended by performance-based codes and manuals presents an efficient solution in terms of computational resources and time for analyzing the consideration of SSI [39, 40]. This method is employed in this study for consideration of SSI

effect and it uses a simplified procedure that considers pull-up effect, and the stiffness of soil and the foundation with accounting for the uncertainties of different site soil classes [41, 42]. Parameters needed for this method are type of soil, capacities, dimension, stiffness and damping ratio of the foundation, also, for calculating the vertical and horizontal bearing capacity of the designed foundation Meyerhof equations were used [23]. Foundations' stiffness was calculated 2-dimensionally according to Gazetas equations considering vertical stiffness along Z-axis, rotational stiffness along Y-axis and horizontal stiffness along X-axis are required, and more importantly sum of vertical and total rotational stiffness of the employed springs were respectively equal to total elastic stiffness and the sum of rotational stiffness produced via vertical springs along the footing which confirmed the correct assignment of the SSI properties [23]. Also, due to insensitivity of BNWF method on horizontal distance of the springs (not mesh sensitive), springs were positioned with a 25 cm distance [23]. In addition, it must be noted that the soil properties were assigned to the predefined springs in OpenSees using two nonlinear material models of Qzsimple and Tzsimple which respectively are capable of modeling the load-displacement and shear-sliding behavioral curves. For this purpose, material models of Qzsimple and Tzsimple were assigned to the vertical and horizontal degrees of freedom of the zero length elements "ZeroLength" which practically were implemented as the vertical and horizontal Winkler springs along the footing [23].

Based on the procedure and details discussed, simulation of the investigated models was performed by OpenSees software [38]. Considered seismic mass of models were set equal to 1.05DL + 0.5LL [23]. Designed models were simulated 2-dimensionally in OpenSees in which a circumferential moment-resisting frame from each model is selected for simulation. To account for the third dimension, the "P- Δ column" or "leaning column" was added to 2D models [43-45]. Using this technique, each floor's mass is calculated and applied to the elemental nodes. Shown in Figure 2, gravity columns are located in a row with hinge joints at the right side of frame being connected to the structure using "truss" elements, section area and moment of inertia of gravity columns are equal to the eliminated columns from the 3D model [23]. Also, in the numerical simulation using OpenSees software [38], cyclic degradation is considered and it is part of the material assignment procedure. The "uniaxialMaterialSteel02" attribute in OpenSees has the cyclic material degradation consideration embedded within itself which was assigned as steel material property to the structural element [23].

In addition, to validate the simulated models two steps are accomplished, at the first step to verify the linear behaviour the fundamental periods of the simulated models and designed ones are compared. In the second step, to verify the nonlinear behaviour an experimental test is used as a benchmark for validating the results of the simulated models. However, since the investigated models in this study are the same as the ones used in another research paper by the authors [23] in which they have been validated and proved to have satisfied both the linear and nonlinear validation, more description regarding the validation procedure is available in the mentioned paper [23].

2.6. Development of Fragility Curves

Fragility curves as an efficient approach for considering uncertainties in the analytical interpretation of seismic performance assessment of structures are quite in demand. As discussed in previous sections, IDA curves are used for the development of the fragility curves, but it has to be noted that the first stage of this procedure is understanding the inputs and outputs, a parameter named intensity measure (IM) must be chosen by a seismic risk analysis of the desired region to be applied to the structure, and at the subsequent stage a corresponding structural response to each Damage Measure (DM) is achieved which would be considered as an Engineering Demand Parameter (EDM), and finally based on a pre-defined damage indicator, collapse probability can be calculated which can be used for cost estimation of structural rehabilitation. So, IDA Curves are a set of IM-EDP graphs by which probabilistic studies can be accomplished [23].

IM is a scalable quantity of a record, in this study records' spectral acceleration corresponding to the first mode of the structure with a damping ratio of 5% ($S_{a(T1,\ 5\%)}$) were chosen to be more efficient to be used as the correct input for extracting the IDA Curves because they have far less data scattering compared with other quantities like PGA. Regarding the DM as the output of the IDA procedure, the maximum inter-storey drift ratio is the chosen DM used for the analysis of IDA curves [23].

To achieve fragility curves, the corresponding EDPs to each IM in the nonlinear dynamic analysis, a probabilistic distribution must be collected. Considering the standard and mean deviation for each EDP and subsequently using the cumulative distribution function, exceeding probability can be calculated [46].

$P(C/IM = X)$ indicates the probability of exceeding a performance level at a specified IM [46]:

$$P(C/IM = X) = \Phi\left(\frac{\ln(x/\theta)}{\beta}\right) \qquad (1)$$

$$\ln(\theta) = \frac{1}{n}\sum_{i-1}^{n} \ln(IM_i) \qquad (2)$$

$$\beta = \sqrt{\frac{1}{n-1}\sum_{i-1}^{n} \left(\ln\left(\frac{IM_i}{\theta}\right)\right)^2} \qquad (3)$$

In which, θ is the mean of the fragility function (IM level with 50% probability) and β is the standard deviation of Ln(IM)

Equation 1 presents values of IM which correspondingly exceed a performance level at a specified IM. These values have Normal Distribution.

The probability of exceeding from performance levels of IO, LS, and CP are set to change between 0 to 1, and the maximum drift value reaching each of these three levels respectively are

considered 0.7%H (0.007H), 2.5%H (0.025H) and 5% (0.05H) in which H is the storey height [47].

Targeted fragility curves for the seismic safety assessment of the models considering the specified performance levels can be produced by IDA curves ($S_{a(T1,5\%)}$ − Drift $_{Max}$ (%H)) scaled to $S_{a(Design)}$ and then utilizing Normal Probability Distribution corresponding to maximum drift values based on specified IM.

3. Discussion of the results

3.1. IDA Curves

IDA curves resulted from the analysis must be scaled and uniformed, Figure 3 shows an example of the resulted unscaled IDA curves of a 3-storey model with flexible base which presents the behaviour of the model under subjection of far-field records. Resulted and scaled ($S_{a(T1,5\%)}/S_{a(Design)}$ − Drift $_{Max}$ (%H)) IDA curves of the 3, 6, and 9-storey models with and without SSI consideration are shown in Figures 4 to 6. In these figures, uniformed IDA curves (50%) scaled to $S_{a(Design)}$ for three investigated models with fixed base and flexible base considering all three site soil classes are depicted in which they are divided based on the ground motion record type used in the IDA procedure. Generally, assessment of these curves shows that in all the models with or without SSI consideration and under three ground motion types, site soil class D has contributed to lower $S_{a(T1,5\%)}/S_{a(Design)}$ values as drift increases and almost other site soil classes had no considerable effect on spectral acceleration. Comparing the models, IDA curves resulting from near-field (without pulse) with SSI consideration and site soil class D have lowered the $S_{a(T1,5\%)}/S_{a(Design)}$ values more than other cases, and have tended to reach the performance levels at lower values. Also, figures illustrate that scaled IDA curves of structures with SSI consideration and site soil class D are placed under the curves of structures without SSI consideration and it indicates the unfavorable role of SSI consideration at a specific spectral acceleration, but as the consideration of SSI leads to lower spectral accelerations, it can proceed in reduction of the drifts and formation of internal forces in structural elements. In addition, scaled IDA curves indicate that with the increase of height the value of $S_{a(T1,5\%)}/S_{a(Design)}$ decreases in all the cases.

3.2. Fragility Curves

Extracted fragility curves for the investigated models from different ground motion types with fixed base and flexible base considering all three site soil classes are shown in Figures 7 to 9. Based on the supposed scenario, site soil class C is considered to be the class in which investigated models are initially designed but due to a false interpretation of the geotechnical report there might be an ambiguity in the correct type of site class used for the models, so fragility curves of models with other site soil classes are extracted and compared with the main case which is the case with site soil class C, and overall the SSI consideration versus fixed condition is assessed too.

A note must be discussed regarding the modification of fragility curves for models with site soil class C. The fundamental period of a structure with a flexible base is greater than the one with a

fixed base which implies that SSI consideration decreases the spectral acceleration [23]. In addition, the spectral acceleration $S_{a(T1,5\%)}$ of a case with and without SSI consideration are not equal and inevitably no comparison can be made. Development of fragility curves for cases with and without the SSI consideration shows that the SSI leads to the same collapse criterion at lower spectral accelerations, therefore, to interpret the probability of exceedance of cases with a flexible base, this value has to be checked at lower domains. Fragility curves that are not modified indicate that spectral acceleration of the flexible cases corresponds to higher exceedance probability compared with fixed base cases. To eliminate any wrong interpretation, firstly the collapse spectral accelerations must be revised and then the comparison at equal spectral accelerations can be done.

Also, since the models with the fixed base were initially designed for site soil class C, modification of fragility curves is carried out only for site class C and other curves do not need to be revised.

In addition, it has to be mentioned that comparison and interpretation of calculated collapse probabilities are carried out within the performance level of LS since the specified $S_{a(Design)}$ for each model is located within this performance level, but performance levels of IO and CP respectively are better for models which have lower and higher $S_{a(Design)}$ values than specified $S_{a(Design)}$ of investigated models of this study.

Also, Tables 6 and 7 respectively present the exceedance probability values and summary of the SSI effect on the exceedance probability in terms of percentage.

It can be understood from the fragility curves in Figure 7, Tables 6 and 7 that under far-field ground motion records, SSI consideration with site soil classes B, C, and D within LS performance level respectively has no/decreasing, decreasing, and increasing effect on the exceedance probability of the investigated models. So, comparing the effect of different site soil classes within LS performance level indicates that site soil class D can lead to higher collapse probabilities. Also, under far-field ground motion records, with increasing the height of the models, it seems that for the 9-storey model SSI consideration with site soil classes B and C has the most decreasing effect of -15% on the exceedance probability, while site soil class D has the most increasing effect of +50%.

In the case of models under near-field (without pulse) ground motion records by interpreting Figure 8, Tables 6 and 7, it can be indicated that SSI consideration with site soil classes B, C, and D within LS performance level respectively has decreasing, decreasing and increasing effect on the exceedance probability of the investigated models. By comparison, site soil class D can lead to higher collapse probabilities whereas other classes tend to decrease the collapse probabilities. In addition, under near-field (without pulse) ground motion records, with the variation of the height, SSI consideration with site soil classes B and C has the most decreasing effect of -12.5% on the exceedance probability of the 9-storey model, while site soil class D has the most increasing effect of +15% on the 3-storey model.

Moreover, assessing the results of the investigated models under near-field (with pulse) ground motion records using Figure 9, Tables 6 and 7, it can be perceived that SSI consideration with

site soil classes B, C, and D within LS performance level respectively has decreasing, decreasing and increasing effect on the exceedance probability of the investigated models. By comparison, site soil class D can lead to higher collapse probabilities whereas other classes tend to decrease the collapse probabilities. In addition, under near-field (without pulse) ground motion records, with the variation of the height, SSI consideration with site soil classes B and C has the most decreasing effect of -21.43% on the exceedance probability of the 9-storey model, and site soil class D has the most increasing effect of +35.7%.

3.3. Collapse Margin Ratio

FEMA P-695 [24] defines collapse level ground motions as the intensity that would result in the median collapse of the seismic-force-resisting system. Median collapse occurs when one-half of the structures exposed to this intensity of ground motion would have some form of life-threatening collapse. Collapse level ground motions are higher than MCE (Maximum Considered Earthquake) ground motions. As such, MCE ground motions would result in a comparatively smaller probability of collapse. As defined in the following equation, the collapse margin ratio, CMR, is the ratio of the median 5%-damped spectral acceleration of the collapse level ground motions, $\hat{S}_{CT}$, to the 5%-damped spectral acceleration of the MCE ground motions, S_{MT}, at the fundamental period of the seismic-force-resisting system [48]:

$$\mathrm{CMR} = \frac{\hat{S}_{CT}}{S_{MT}} \qquad (4)$$

In one sense, the collapse margin ratio (CMR), could be thought of as the amount of S_{MT} that must be increased to achieve building collapse by 50% of the ground motions. Figure 10 shows the calculated CMR of the investigated models in a comparative chart. It can be understood that under far-field ground motion records SSI consideration with site soil classes B, C, and D tend to respectively have negligible decreasing, decreasing, and increasing effects on the CMR values. In the case of near-field (without pulse) ground motion records SSI consideration with site soil classes B, C, and D indicate to have scattered effects versus height variation, showing no effect or negligible effect on the CMR values. Finally, SSI consideration with site soil classes B, C, and D shows to respectively have no effect, negligible decreasing or increasing effect on the CMR values. Overall, it can be concluded that SSI consideration in flexible cases does not tend to considerably change the CMR values compared with the cases of a fixed base.

4. Summary and Conclusions

In this paper, the effect of various site soil classes on the structural exceedance probability was investigated. The considered problem was how much an incorrect assumption for soil type may endanger the seismic safety of moment-resisting steel frame structures. To this aim, a set of moment-resisting steel frame structures were designed for the site soil class of C, but later on, the site soil classification turns out to be inaccurate. So, 2D models of the considered structures with flexible foundations initially designed for the site soil class of C were analyzed the using IDA method subjected to far-field, near-field (with pulse), and near-field (without pulse) ground motion records of FEMA-P695. For investigating the effect of false site soil class on the exceedance probability of the models, two other soil classes B and D were used in the SSI specification of the initially designed models. Subsequently, fragility curves were developed for

each model under each ground motion record type and the collapse margin ratio for each model was calculated. The results are summarized as follows:

1. Assessment of IDA curves showed that in all the models with or without SSI consideration and under three ground motion types, site soil class D has contributed to lower $S_{a(T1,5\%)}/S_{a(Design)}$ values as drift increases and almost other site soil classes had no considerable effect on spectral acceleration.

2. Fragility curves extracted from far-field ground motion records showed that SSI consideration in all the models does affect the exceedance probability. Soil classes B and C had a decreasing effect while site soil class D had an increasing effect on the exceedance probability. It must be noted that for the 9-storey model, site soil class D had an increasing 50% effect within the LS performance level on the exceedance probability. So, in the assumed scenario of false interpretation of the geotechnical report, if the real site soil class turns out to be class D while the 9-storey model is designed for class C, this false assumption is significant.

3. The fragility curves extracted from the near-field without pulse ground motion records showed that SSI consideration in all the models does affect the exceedance probability. Site soil classes B and C had decreasing effect while site soil class D had an increasing effect on the exceedance probability. Also, it must be emphasized that for the 3-story model, the site soil class D had an increasing 15% effect within the LS performance level on the exceedance probability. So, in the assumed scenario of false interpretation of the geotechnical report, if the real site soil class turns out to be class D while the 3-story model is designed for class C, this false assumption may not be very significant.

4. The fragility curves extracted from near-field with pulse ground motion records showed that SSI consideration in all the models does affect the exceedance probability and site soil classes B and C had decreasing effect while site soil class D had an increasing effect on the exceedance probability. Also, it must be emphasized that for the 9-story model site soil class D had an increasing 35.7% effect within LS performance level on the exceedance probability. So, in the assumed scenario of false interpretation of the geotechnical report, if the real site soil class turns out to be class D while the 9-storey model is designed for class C, this false assumption is significant.

5. Evaluating all the investigated models, SSI consideration in flexible cases does not considerably change the CMR values under all three ground motion record types.

6. Based on the investigated models, it can be concluded that in the assumed scenario of false interpretation of the geotechnical report, if the site soil class B is the accurate class while the structure is designed for class C, then it does not have a negative effect on the exceedance probability. But, if it turns out that the real site soil class is class D, then it can significantly affect the exceedance probability, especially in higher-rising structures.

It can be suggested for the future research topics to follow the same scenarios in this study but with different structural models in terms of structural system, storey number, and geometrical

details. Also, it is suggested to study the effect of foundation failure under inaccurate site soil class consideration more in detail using time-history methods to be able to capture the residual deformations in the structural members but more importantly, being able to analyze the rate of soil failure under the foundation.

References

1. Littlejohn, G.S., Arber, N.R., Craig, C. and Forde, M.C. "Inadequate site investigation" Instn Civ. Engrs, p.1, (1991).

2. Hu, Y. and Wang, Y. "Probabilistic soil classification and stratification in a vertical cross-section from limited cone penetration tests using random field and Monte Carlo simulation" Computers and Geotechnics, **124**, p.103634, (2020).

3. Hytiris, N., Stott, R. and McInnes, K. "The importance of site investigation in the construction industry: a lesson to be taught to every graduate civil and structural engineer" World Transactions on Engineering and Technology Education, **12(3)**, pp.414-419, (2014).

4. Wang, X. "Uncertainty quantification and reduction in the characterization of subsurface stratigraphy using limited geotechnical investigation data" Underground Space, **5(2)**, pp.125-143, (2020).

5. Li, J., Cai, Y., Li, X. and Zhang, L. "Simulating realistic geological stratigraphy using direction-dependent coupled Markov chain model" Computers and Geotechnics, **115**, p.103147, (2019).

6. Gong, W., Zhao, C., Juang, C.H., Tang, H., Wang, H. and Hu, X. "Stratigraphic uncertainty modelling with random field approach" Computers and Geotechnics, **125**, p.103681, (2020).

7. Gong, W., Juang, C.H. and Wasowski, J. "Geohazards and human settlements: Lessons learned from multiple relocation events in Badong, China–Engineering geologist's perspective" Engineering Geology, **285**, p.106051, (2021).

8. Phoon, K. K., Cao, Z. J., Ji, J., Leung, Y. F., Najjar, S., Shuku, Tang, C., Yin, Z.Y., Ikumasa, Y. and Ching, J. "Geotechnical uncertainty, modeling, and decision making" Soils and Foundations, **62(5)**, p.101189, (2022).

9. Crisp, M. P., Jaksa, M., and Kuo, Y. "Optimal testing locations in geotechnical site investigations through the application of a genetic algorithm" Geosciences, **10(7)**, p.265, (2020).

10. Crisp, M. P., Jaksa, M. B., and Kuo, Y. L. "Effect of borehole location on pile performance" Georisk: Assessment and Management of Risk for Engineered Systems and Geohazards, pp.1-16, (2020).

11. Otake, Y., and Honjo, Y. "Challenges in geotechnical design revealed by reliability assessment: Review and future perspectives" Soils and Foundations, **62(3)**, p.101129, (2022).

12. Fernandes, I., and Chaminé, H. I. "In situ geotechnical investigations" Advances on Testing and Experimentation in Civil Engineering, pp.29-54, (2023).

13. Crisp, M. P., Jaksa, M. B., and Kuo, Y. L. "Towards Optimal Site Investigations for Generalized Structural Configurations" In Proceedings of the 7th International Symposium on Geotechnical Safety and Risk, Taipei, Taiwan, pp.11-13, (2019).

14. Jaksa, M. B., Goldsworthy, J. S., Fenton, G. A., Kaggwa, W. S., Griffiths, D. V., Kuo, Y. L., and Poulos, H. G. "Towards reliable and effective site investigations" Géotechnique, **55(2)**, pp.109-121, (2005).

15. Guan, Z., and Wang, Y. "Statistical charts for determining sample size at various levels of accuracy and confidence in geotechnical site investigation" Géotechnique, **70(12)**, pp.1145-1159, (2020).

16. Goldsworthy, J. S., Jaksa, M. B., Kaggwa, W. S., Fenton, G. A., Griffiths, D. V., and Poulos, H. G. "Cost of foundation failures due to limited site investigations" The International Conference on Structural and Foundation Failures, pp. 2-4, (2004).

17. Clayton, C. R. "Managing geotechnical risk: improving productivity in UK building and construction" Thomas Telford, (2001).

18. Wang, Y., and Li, P. "Data-driven determination of sample number and efficient sampling locations for geotechnical site investigation of a cross-section using Voronoi diagram and Bayesian compressive sampling" Computers and Geotechnics, **130**, p.103898, (2021).

19. Crisp, M. P., Jaksa, M. B., and Kuo, Y. L. "Characterising site investigation performance in multiple-layer soils and soil lenses" Georisk: Assessment and Management of Risk for Engineered Systems and Geohazards, **15(3)**, pp.196-208, (2021).

20. Crisp, M. P., Jaksa, M. B., Kuo, Y. L., Fenton, G. A., and Griffiths, D. V. "Characterizing site investigation performance in a two-layer soil profile" Canadian Journal of Civil Engineering, **48(2)**, pp.115-123, (2021).

21. Zhao, C., Gong, W., Li, T., Juang, C. H., Tang, H., and Wang, H. "Probabilistic characterization of subsurface stratigraphic configuration with modified random field approach" Engineering Geology, **288**, p.106138, (2021).

22. Vamvatsikos, D., and Cornell, C. A. "Incremental dynamic analysis" Earthquake engineering & structural dynamics, **31(3)**, pp.491-541, (2002).

23. Sabouniaghdam, M., Mohammadi Dehcheshmeh, E., Safari, P., Broujerdian, V. "Probabilistic collapse assessment of steel frame structures considering the effects of soil-structure interaction and height" Scientia Iranica, **29(6)**, pp. 2979-2994, (2022).

24. ATC "Quantification of building seismic performance factors" US Department of Homeland Security, FEMA, (2009).

25. Akhoondi, M. R., and Behnamfar, F. "Seismic fragility curves of steel structures including soil-structure interaction and variation of soil parameters" Soil Dynamics and Earthquake Engineering, **143**, p.106609, (2021).

26. Karafagka, S., Fotopoulou, S., and Pitilakis, D. "Fragility curves of non-ductile RC frame buildings on saturated soils including liquefaction effects and soil–structure interaction" Bulletin of Earthquake Engineering, **19(15)**, pp.6443-6468, (2021).

27. Petridis, C., and Pitilakis, D. "Fragility curve modifiers for reinforced concrete dual buildings, including nonlinear site effects and soil–structure interaction" Earthquake Spectra, **36(4)**, pp.1930-1951, (2020).

28. Tahghighi, H., and Mohammadi, A. "Numerical evaluation of soil–structure interaction effects on the seismic performance and vulnerability of reinforced concrete buildings" International Journal of Geomechanics, **20(6)**, p.04020072, (2020).

29. Forcellini, D. "Analytical fragility curves of shallow-founded structures subjected to Soil-Structure Interaction (SSI) effects" Soil Dynamics and Earthquake Engineering, **141**, p.106487, (2021).

30. Hamidia, M., Shokrollahi, N., and Nasrolahi, M. "Soil-structure interaction effects on the seismic collapse capacity of steel moment-resisting frame buildings" Structures, **32**, pp.1331-1345, (2021).

31. Cavalieri, F., Correia, A. A., Crowley, H., and Pinho, R. "Dynamic soil-structure interaction models for fragility characterisation of buildings with shallow foundations" Soil Dynamics and Earthquake Engineering, **132**, p.106004, (2020).

32. Sabermahany, H., Attarnejad, R. "Soil-structure interaction response considering drift analysis due to three orthogonal components of near-field ground motions" Scientia Iranica, **29(6)**, pp.2953-2967, (2022).

33. Tahghighi, H., and Rabiee M. "Influence of foundation flexibility on the seismic response of low-to-mid-rise moment-resisting frame buildings" Scientia Iranica, **24(3)**, pp.979-992, (2017).

34. ASCE standard "Minimum design loads and associated criteria for buildings and other structures" American Society of Civil Engineers, (2017).

35. Verdugo, R. "Seismic site classification" Soil Dynamics and Earthquake Engineering, **124**, pp.317-329, (2019).

36. CSI manual "Analysis reference manual for SAP2000, ETABS, and SAFE" Computers and Structures, Berkeley, California, USA, (2016).

37. Baker, J. W., and Allin Cornell, C. "A vector- valued ground motion intensity measure consisting of spectral acceleration and epsilon" Earthquake Engineering & Structural Dynamics, **34(10)**, pp.1193-1217, (2005).

38. Mazzoni, S., McKenna, F., Scott, M. H., and Fenves, G. L. "OpenSees command language manual" Pacific Earthquake Engineering Research Center, **264(1)**, pp.137-158, (2006).

39. Raychowdhury, P. "Nonlinear Winkler-based shallow foundation model for performance assessment of seismically loaded structures" University of California, San Diego, (2008).

40. Allotey, N., and El Naggar, M. H. "An investigation into the Winkler modeling of the cyclic response of rigid footings" Soil Dynamics and Earthquake Engineering, **28(1)**, pp.44-57, (2008).

41. Gajan, S., Raychowdhury, P., Hutchinson, T. C., Kutter, B. L., and Stewart, J. P. "Application and validation of practical tools for nonlinear soil-foundation interaction analysis" Earthquake Spectra, **26(1)**, pp.111-129, (2010).

42. Harden, C. W. "Numerical modeling of the nonlinear cyclic response of shallow foundations" Pacific Earthquake Engineering Research Center, (2005).

43. Broujerdian, V., and Mohammadi Dehcheshmeh, E. "Locating the rocking section in self-centering bi-rocking walls to achieve the best seismic performance" Bulletin of Earthquake Engineering **20(5)**, pp. 2441-2468, (2022).

44. Ebrahimi Majumerd, M. J., Mohammadi Dehcheshmeh, E., Broujerdian, V., and Moradi, S. "Self-centering rocking dual-core braced frames with buckling-restrained fuses" Journal of Constructional Steel Research **194**, pp.107322 (2022).

45. Mohammadi Dehcheshmeh, E., and Broujerdian, V. "Determination of optimal behavior of self-centering multiple-rocking walls subjected to far-field and near-field ground motions" Journal of Building Engineering **45**, pp. 103509, (2022).

46. Baker, J. W. "Efficient analytical fragility function fitting using dynamic structural analysis", Earthquake Spectra, **31(1)**, pp.579-599, (2015).

47. SAC Joint Venture, Guidelines Development Committee. "Recommended post-earthquake evaluation and repair criteria for welded steel moment-frame buildings", (2000).

48. Mohammadi Dehcheshmeh, E., and Broujerdian, V. "Probabilistic Evaluation of Self-Centering Birocking Walls Subjected to Far-Field and Near-Field Ground Motions", Journal of Structural Engineering **148(9)**, pp. 04022134, (2022).

……

Biographies

Vahid Broujerdian is Assistant Professor of Structural Engineering and Head of Structural Enginnering Group at the School of Civil Engineering at Iran University of Sciecne and Technology. He received his BSc (2002), MSc (2004) and PhD (2010) in Structural Engineering from Sharif University of Technology, Tehran, Iran. His research interests include analytical and numerical study of nonlinear behaviour of materials and structures, design and analysis of wind and earthquake resistant structures, and design and analysis of structures against abnormal conditions (impact, blast and fire).

Esmaeil Mohammadi Dehcheshmeh is Postdoctoral Researcher in Structural and Earthquake Engineering and Research Assistant at Iran University of Science and Technology, Tehran, Iran. He received his BSc (2013) in Civil Engineering from Tabriz University, MSc (2016) and PhD (2022) in Earthquake Engineering from Iran University of Science and Technology. His research interests include design and analysis of new structural systems, seismic resilience of structures, behaviour of structures against abnormal conditions (impact, blast and fire), and using machine learning algorithms to predict seismic behavior of structures.

Pouria Safari is Research Assistant at the Structural Engineering Group of the School of Civil Engineering at Iran University of Science and Technology, Tehran, Iran. He received his BSc (2016) in Civil Engineering from Sharif University of Technology and MSc (2018) in Structural Engineering from Iran University of Science and Technology. His research interests include fire and seismic performance of structures.

……

List of Figure and Table captions:

……

Figures and Tables:

Site Class	**V_{S30} (m/s)**	**N or N_{ch}**	**S_u (kPa)**
B (Rock)	750 – 1500	NA	NA
C (Very Dense Soil and Soft Rock)	360 – 750	> 50	> 96
D (Stiff Soil)	180 – 360	15 – 50	48 – 96

Table 1.

Table 2.

Structures	Stories	MRF Column	Gravity Column	MRF Beam	Gravity Beam	Secondary Beam	Foundations	
							Width×Length×Height	Depth
3-storey	1^{st}	IPB320	IPB180	IPE400	IPE330	IPE220	$1 \times 16 \times 0.7$ m^3	1.2 m
	2^{nd}	IPB280	IPB160	IPE360	IPE330	IPE220		
	3^{rd}	IPB220	IPB140	IPE330	IPE330	IPE220		
6-storey	$1^{st} – 2^{nd}$	IPB400	IPB240	IPE500	IPE330	IPE220	$1.5 \times 16.5 \times 1.0$ m^3	1.5 m
	$3^{rd} – 4^{th}$	IPB320	IPB180	IPE450	IPE330	IPE220		
	$5^{th} – 6^{th}$	IPB280	IPB160	IPE360	IPE330	IPE220		
9-storey	$1^{st} – 3^{rd}$	IPB550	IPB320	IPE550	IPE330	IPE220	$2 \times 17 \times 1.3$ m^3	1.8 m
	$4^{th} – 6^{th}$	IPB400	IPB240	IPE500	IPE330	IPE220		
	$7^{th} – 9^{th}$	IPB320	IPB180	IPE400	IPE330	IPE220		

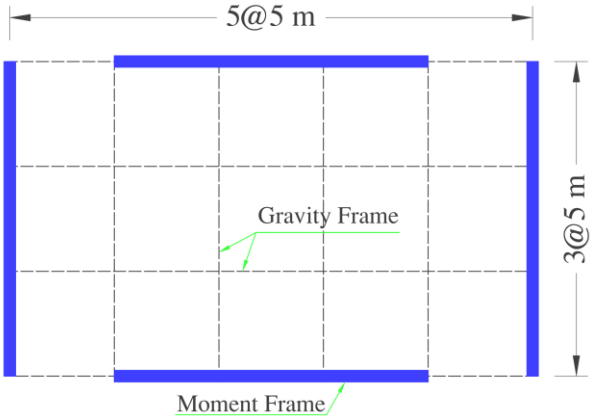

(a) Plan View

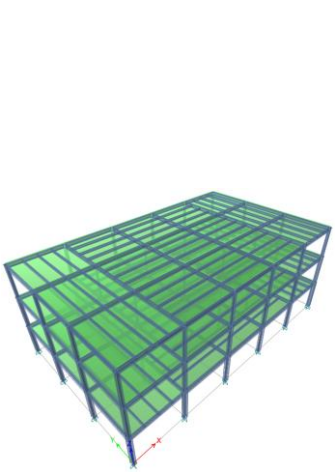

(b) 3-Storey

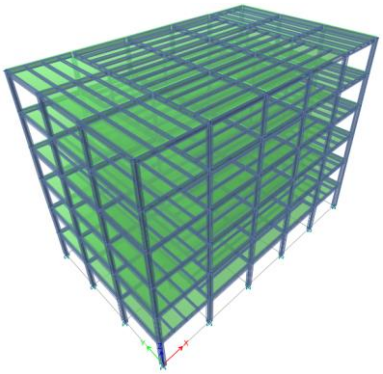

(c) 6-Storey

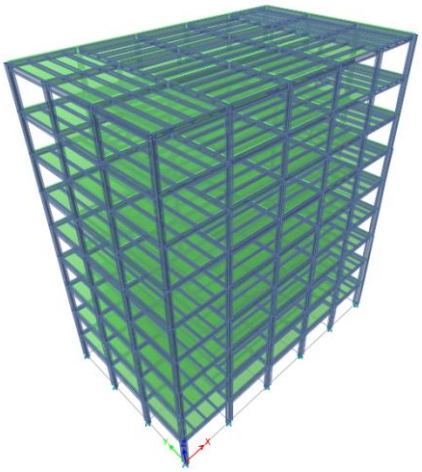

(d) 9-Storey

Figure 1.

Table 3.

Far-Field					
No.	**RSN***	**Name**	**M (Richter)**	**PGA_{max} (g)**	**PGV_{max} (cm/s)**
1	953	Northridge-01	6.7	0.52	63
2	960	Northridge-01	6.7	0.48	45
3	1602	Duzce, Turkey	7.1	0.82	62
4	1787	Hector Mine	7.1	0.34	42
5	169	Imperial Valley-06	6.5	0.35	33
6	174	Imperial Valley-06	6.5	0.38	42
7	1111	Kobe, Japan	6.9	0.51	37
8	1116	Kobe, Japan	6.9	0.24	38
9	1158	Kocaeli, Turkey	7.5	0.36	59
10	1148	Kocaeli, Turkey	7.5	0.22	40
11	900	Landers	7.3	0.24	52
12	848	Landers	7.3	0.42	42
13	752	Loma Prieta	6.9	0.53	35
14	767	Loma Prieta	6.9	0.56	45
15	1633	Manjil, Iran	7.4	0.51	54
16	721	Superstition Hills-02	6.5	0.36	46
17	725	Superstition Hills-02	6.5	0.45	36
18	827	Cape Mendocino	7.0	0.55	44
19	1244	Chi-Chi, Taiwan	7.6	0.44	115
20	1485	Chi-Chi, Taiwan	7.6	0.51	39
21	68	San Fernando	6.6	0.21	19
22	125	Friuli, Italy-01	6.5	0.35	31

* Record Serial Number

Table 4.

Near-Field (With Pulse)					
No.	**RSN***	**Name**	**M (Richter)**	**PGA_{max} (g)**	**PGV_{max} (cm/s)**
1	181	Imperial Valley-06	6.5	0.44	111.9
2	182	Imperial Valley-06	6.5	0.46	108.9
3	292	Irpinia, Italy-01	6.9	0.31	45.5
4	723	Superstition-Hills-02	6.5	0.42	106.8
5	802	Loma Prieta	6.9	0.38	55.6
6	821	Erzican, Turkey	6.7	0.49	95.5
7	828	Cape Mendocino	7.0	0.63	82.1
8	879	Landers	7.3	0.79	140.3
9	1063	Northridge-01	6.7	0.87	169.3
10	1086	Northridge-01	6.7	0.73	122.8
11	1165	Kocaeli, Turkey	7.5	0.22	29.8
12	1503	Chi-Chi, Taiwan	7.6	0.82	127.7
13	1529	Chi-Chi, Taiwan	7.6	0.29	106.6
14	1605	Duzce, Turkey	7.1	0.52	79.3

*** Record Serial Number**

Table 5.

Near-Field (Without Pulse)					
No.	**RSN***	**Name**	**M (Richter)**	**PGA_{max} (g)**	**PGV_{max} (cm/s)**
1	126	Gazli, USSR	6.8	0.71	71.2
2	160	Imperial Valley-06	6.5	0.76	44.3
3	165	Imperial Valley-06	6.5	0.28	30.5
4	495	Nahanni, Canada	6.8	1.18	43.9
5	496	Nahanni, Canada	6.8	0.45	34.7
6	741	Loma Prieta	6.9	0.64	55.9
7	753	Loma Prieta	6.9	0.51	45.5
8	825	Cape Mendocino	7.0	1.43	119.5
9	1004	Northridge-01	6.7	0.73	70.1
10	1048	Northridge-01	6.7	0.42	53.2
11	1176	Kocaeli, Turkey	7.5	0.31	73
12	1504	Chi-Chi, Taiwan	7.6	0.56	91.8
13	1517	Chi-Chi, Taiwan	7.6	1.16	115.1
14	2114	Denali, Alaska	7.9	0.33	126.4

*** Record Serial Number**

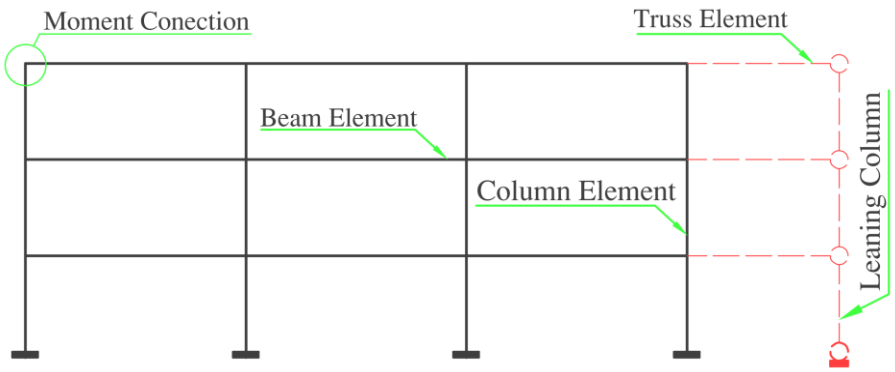
Moment Conection
Truss Element
Beam Element
Column Element
Leaning Column

Figure 2.

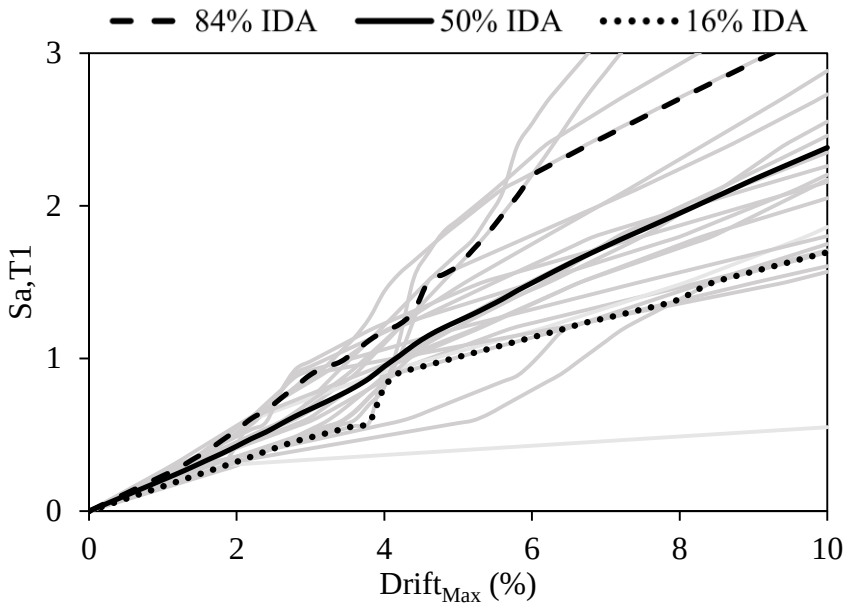

Figure 3.

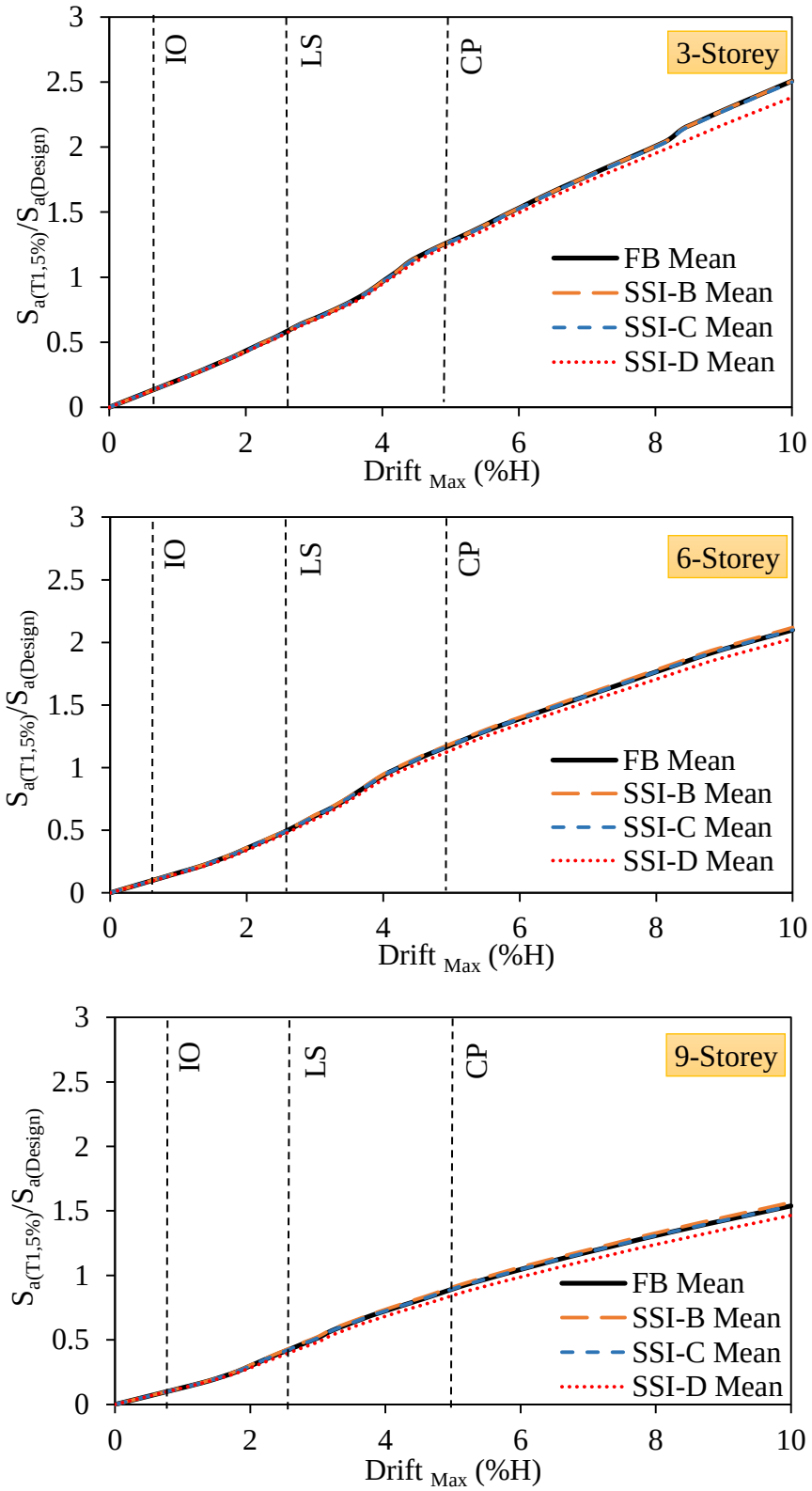
3-Storey
IO
LS
CP
FB Mean
SSI-B Mean
SSI-C Mean
SSI-D Mean
$S_{a(T1,5\%)}/S_{a(Design)}$
Drift $_{Max}$ (%H)
6-Storey
9-Storey

Fig. 4

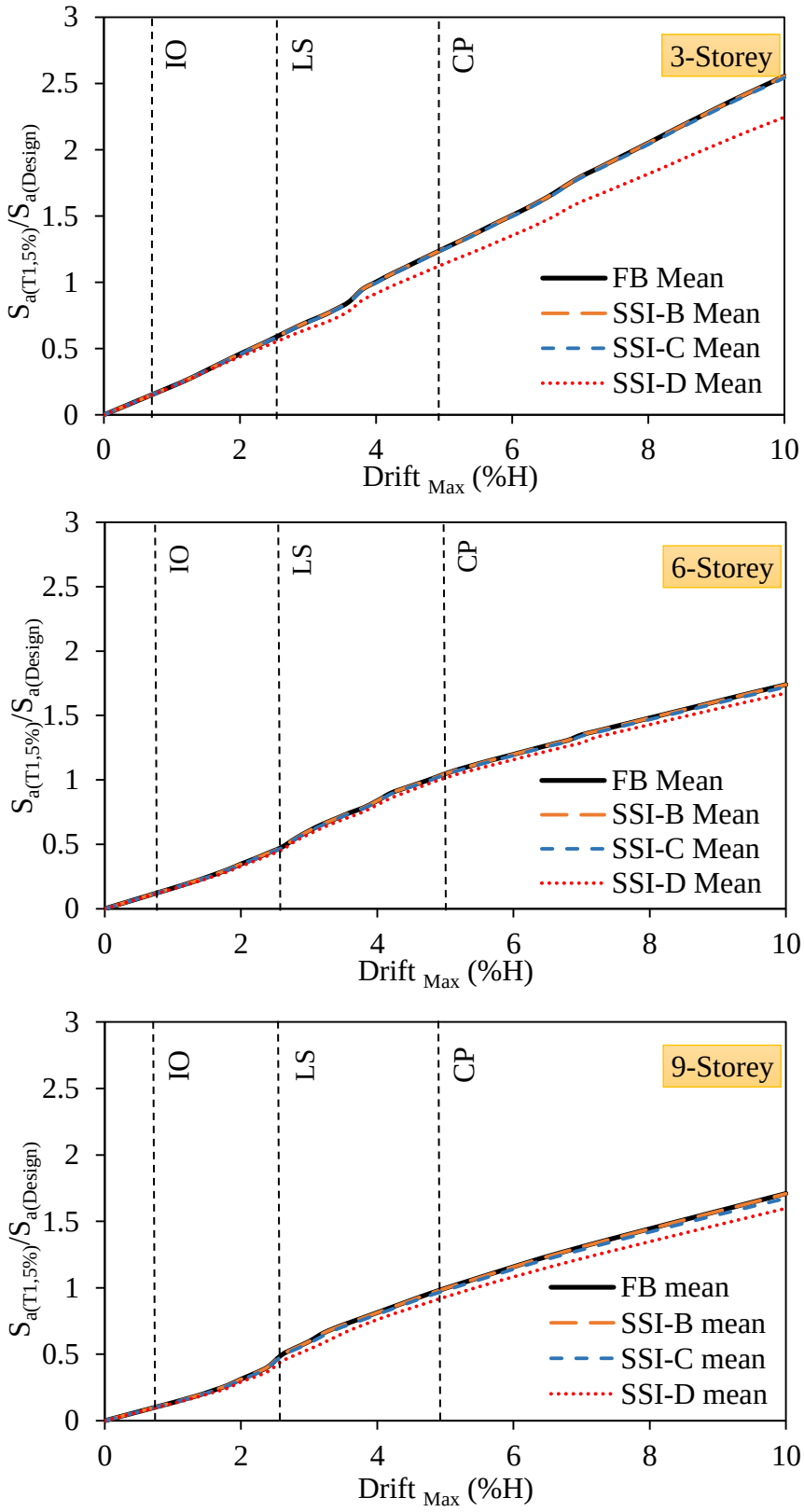
3-Storey
IO
LS
CP
FB Mean
SSI-B Mean
SSI-C Mean
SSI-D Mean
$S_{a(T1,5\%)}/S_{a(Design)}$
Drift $_{Max}$ (%H)
6-Storey
IO
LS
CP
FB Mean
SSI-B Mean
SSI-C Mean
SSI-D Mean
$S_{a(T1,5\%)}/S_{a(Design)}$
Drift $_{Max}$ (%H)
9-Storey
IO
LS
CP
FB mean
SSI-B mean
SSI-C mean
SSI-D mean
$S_{a(T1,5\%)}/S_{a(Design)}$
Drift $_{Max}$ (%H)

Fig. 5

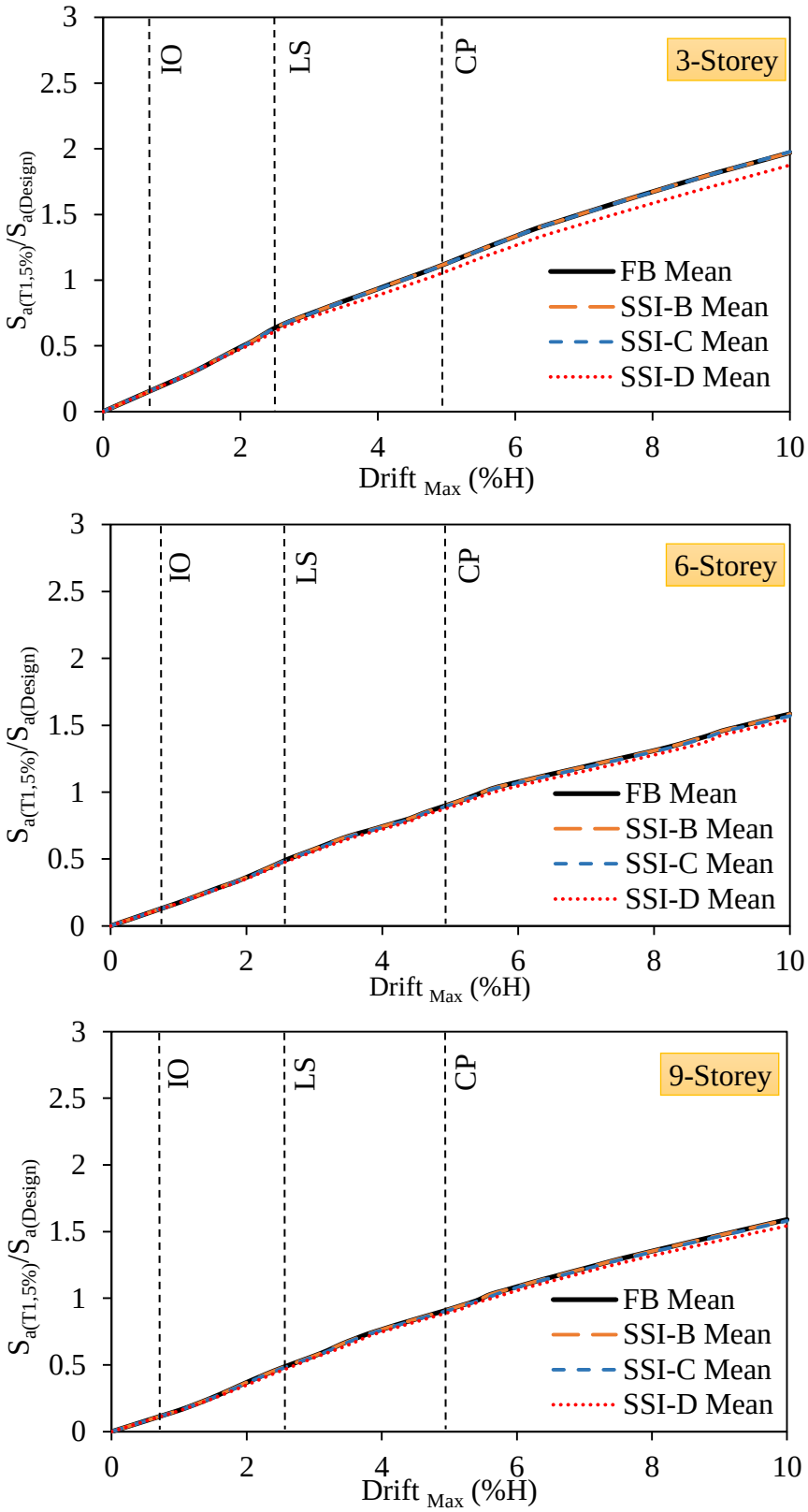
3-Storey
6-Storey
9-Storey
IO
LS
CP
FB Mean
SSI-B Mean
SSI-C Mean
SSI-D Mean
$S_{a(T1,5\%)}/S_{a(Design)}$
Drift $_{Max}$ (%H)
0
0.5
1
1.5
2
2.5
3
0
2
4
6
8
10

Fig. 6

Table 6.

Exceedance Probability										
	Investigated Models		Far-Field Records			Near-Field (Without Pulse)			Near-Field (With Pulse)		
			3-Storey	6-Storey	9-Storey	3-Storey	6-Storey	9-Storey	3-Storey	6-Storey	9-Storey
Performance Levels	IO	Fixed Base	1	1	1	1	1	1	1	1	1
		SSI-B	1	1	1	1	1	1	1	1	1
		SSI-C	1	1	1	1	1	1	1	1	1
		SSI-C-mod	1	1	1	1	1	1	1	1	1
		SSI-D	1	1	1	1	1	1	1	1	1
	LS	Fixed Base	0.8	0.63	0.1	0.67	0.64	0.2	0.7	0.68	0.14
		SSI-B	0.8	0.63	0.095	0.65	0.62	0.19	0.68	0.67	0.13
		SSI-C	0.75	0.62	0.09	0.64	0.6	0.18	0.67	0.65	0.125
		SSI-C-mod	0.7	0.60	0.085	0.6	0.58	0.175	0.65	0.63	0.11
		SSI-D	0.82	0.7	0.15	0.77	0.7	0.21	0.71	0.7	0.19
	CP	Fixed Base	0.037	0.022	0.01	0.03	0.08	0.01	0.04	0.01	0.01
		SSI-B	0.035	0.02	0.0095	0.028	0.077	0.0095	0.037	0.0095	0.009
		SSI-C	0.033	0.018	0.009	0.027	0.075	0.009	0.036	0.009	0.0075
		SSI-C-mod	0.03	0.015	0.008	0.026	0.07	0.008	0.03	0.0085	0.007
		SSI-D	0.04	0.025	0.012	0.12	0.09	0.011	0.04	0.012	0.0105

SSI Effect on the Exceedance Probability (+/-%)									
Cases	**Far-Field Records**			**Near-Field (Without Pulse)**			**Near-Field (With Pulse)**		
	3-Storey	**6-Storey**	**9-Storey**	**3-Storey**	**6-Storey**	**9-Storey**	**3-Storey**	**6-Storey**	**9-Storey**
SSI-B	0	0	-5	-3	-3.125	-5	-2.86	-1.47	-7.14
SSI-C-mod	-12.5	-4.76	-15	-10.45	-9.375	-12.5	-7.14	-7.35	-21.43
SSI-D	+2.5	+11.11	+50	+15	+9.375	+5	+1.43	+2.94	+35.7

Table 7.

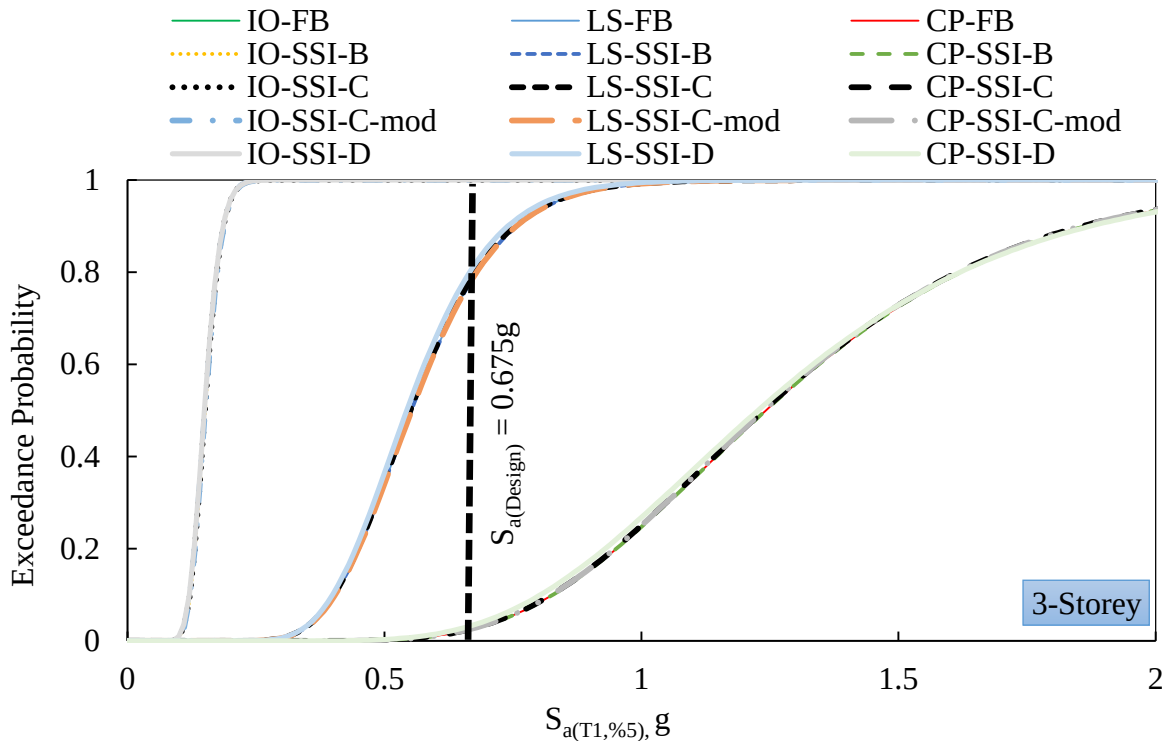
IO-FB
LS-FB
CP-FB
IO-SSI-B
LS-SSI-B
CP-SSI-B
IO-SSI-C
LS-SSI-C
CP-SSI-C
IO-SSI-C-mod
LS-SSI-C-mod
CP-SSI-C-mod
IO-SSI-D
LS-SSI-D
CP-SSI-D
Exceedance Probability
0
0.2
0.4
0.6
0.8
1
0
0.5
1
1.5
2
$S_{a(T1,\%5)}$, g
$S_{a(Design)}$ = 0.675g
3-Storey

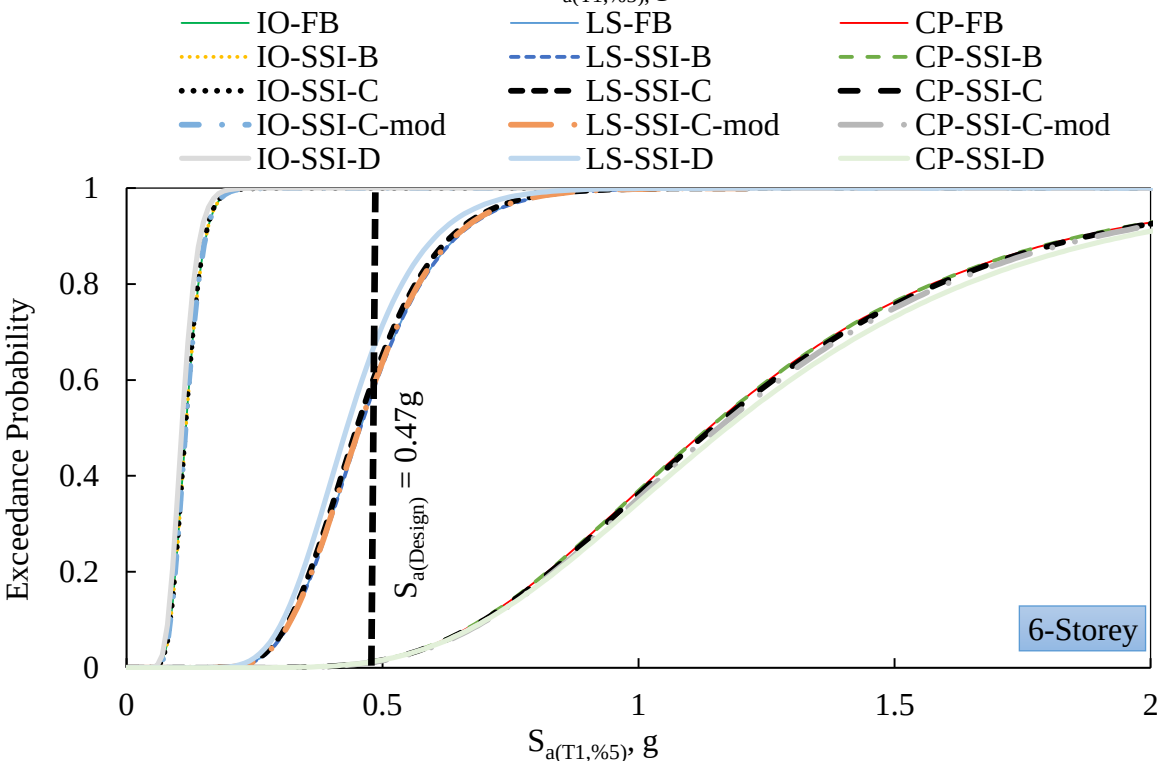
IO-FB
LS-FB
CP-FB
IO-SSI-B
LS-SSI-B
CP-SSI-B
IO-SSI-C
LS-SSI-C
CP-SSI-C
IO-SSI-C-mod
LS-SSI-C-mod
CP-SSI-C-mod
IO-SSI-D
LS-SSI-D
CP-SSI-D
Exceedance Probability
0
0.2
0.4
0.6
0.8
1
0
0.5
1
1.5
2
$S_{a(T1,\%5)}$, g
$S_{a(Design)}$ = 0.47g
6-Storey

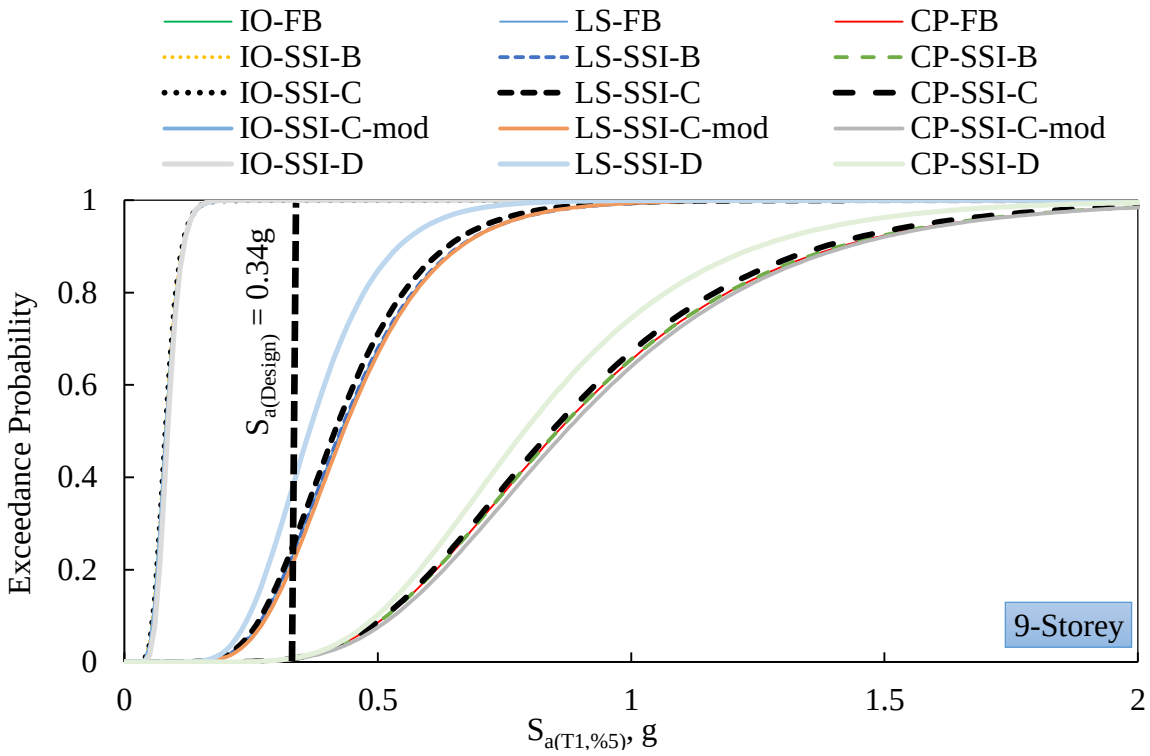
IO-FB
LS-FB
CP-FB
IO-SSI-B
LS-SSI-B
CP-SSI-B
IO-SSI-C
LS-SSI-C
CP-SSI-C
IO-SSI-C-mod
LS-SSI-C-mod
CP-SSI-C-mod
IO-SSI-D
LS-SSI-D
CP-SSI-D
Exceedance Probability
1
0.8
0.6
0.4
0.2
0
$S_{a(Design)}$ = 0.34g
0
0.5
1
1.5
2
$S_{a(T1,\%5)}$, g
9-Storey

Figure 7.

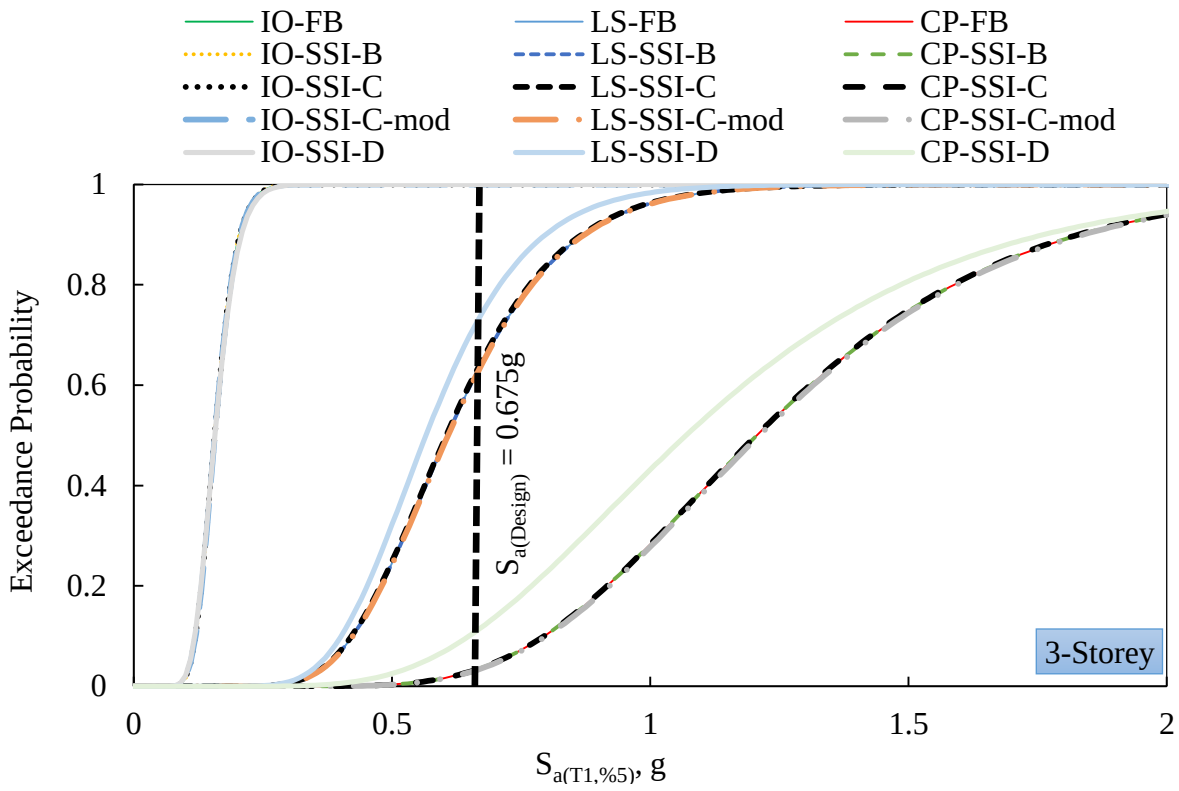
IO-FB
LS-FB
CP-FB
IO-SSI-B
LS-SSI-B
CP-SSI-B
IO-SSI-C
LS-SSI-C
CP-SSI-C
IO-SSI-C-mod
LS-SSI-C-mod
CP-SSI-C-mod
IO-SSI-D
LS-SSI-D
CP-SSI-D
Exceedance Probability
0
0.2
0.4
0.6
0.8
1
0
0.5
1
1.5
2
$S_{a(T1,\%5)}$, g
$S_{a(Design)}$ = 0.675g
3-Storey

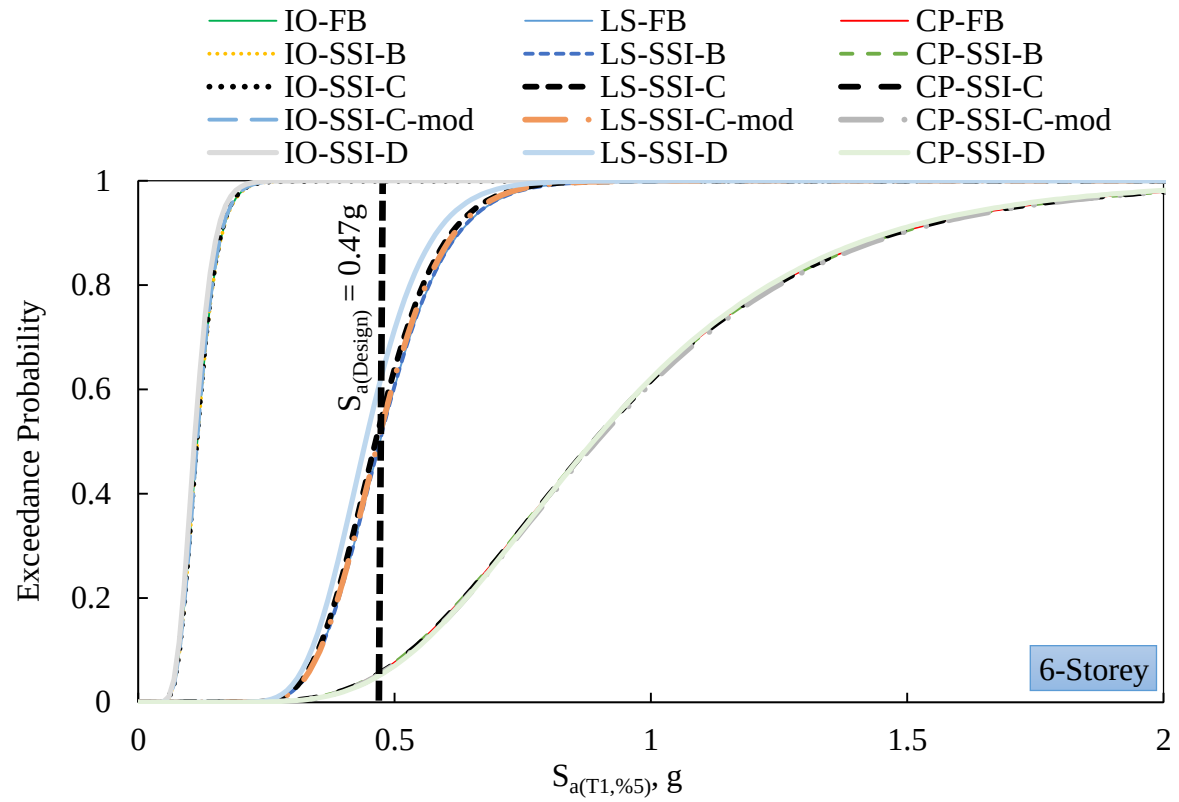
IO-FB
LS-FB
CP-FB
IO-SSI-B
LS-SSI-B
CP-SSI-B
IO-SSI-C
LS-SSI-C
CP-SSI-C
IO-SSI-C-mod
LS-SSI-C-mod
CP-SSI-C-mod
IO-SSI-D
LS-SSI-D
CP-SSI-D
Exceedance Probability
0
0.2
0.4
0.6
0.8
1
0
0.5
1
1.5
2
$S_{a(T1,\%5)}$, g
$S_{a(Design)}$ = 0.47g
6-Storey

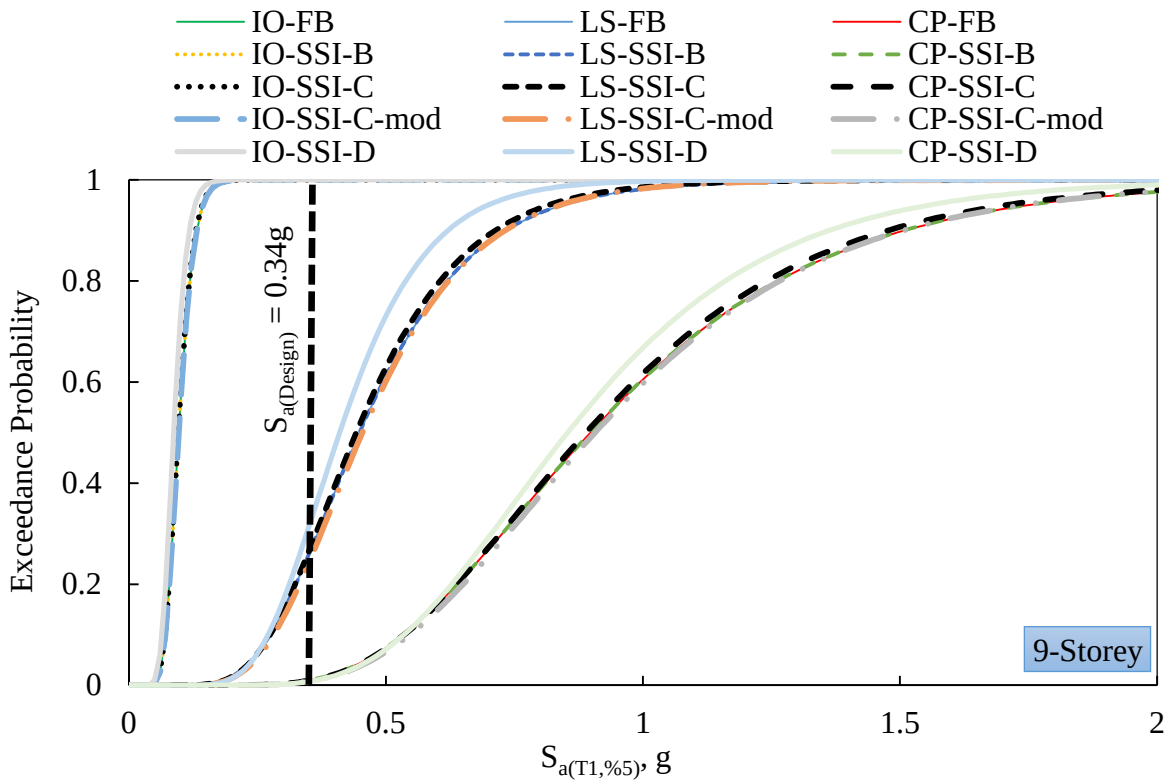
IO-FB
LS-FB
CP-FB
IO-SSI-B
LS-SSI-B
CP-SSI-B
IO-SSI-C
LS-SSI-C
CP-SSI-C
IO-SSI-C-mod
LS-SSI-C-mod
CP-SSI-C-mod
IO-SSI-D
LS-SSI-D
CP-SSI-D
Exceedance Probability
1
0.8
0.6
0.4
0.2
0
0
0.5
1
1.5
2
$S_{a(Design)}$ = 0.34g
$S_{a(T1,\%5)}$, g
9-Storey

Figure 8.

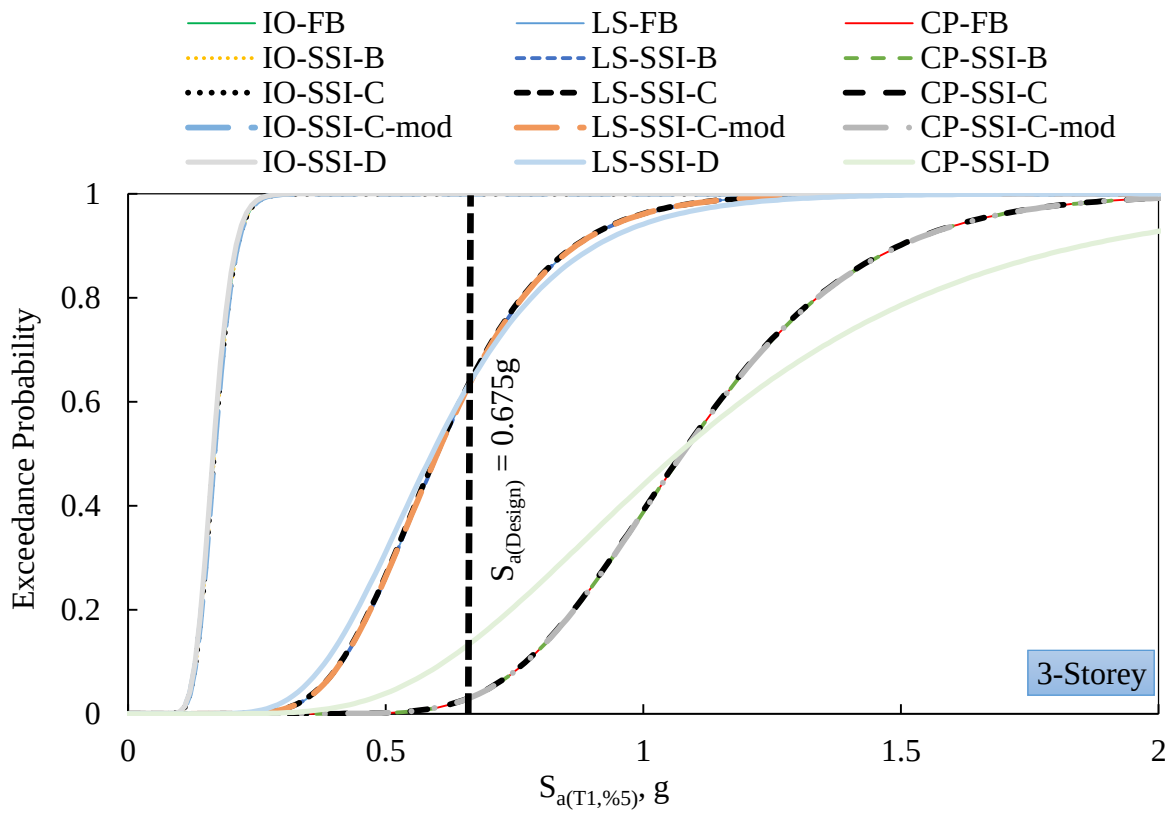
IO-FB
LS-FB
CP-FB
IO-SSI-B
LS-SSI-B
CP-SSI-B
IO-SSI-C
LS-SSI-C
CP-SSI-C
IO-SSI-C-mod
LS-SSI-C-mod
CP-SSI-C-mod
IO-SSI-D
LS-SSI-D
CP-SSI-D
Exceedance Probability
0
0.2
0.4
0.6
0.8
1
0
0.5
1
1.5
2
$S_{a(T1,\%5)}$, g
$S_{a(Design)}$ = 0.675g
3-Storey

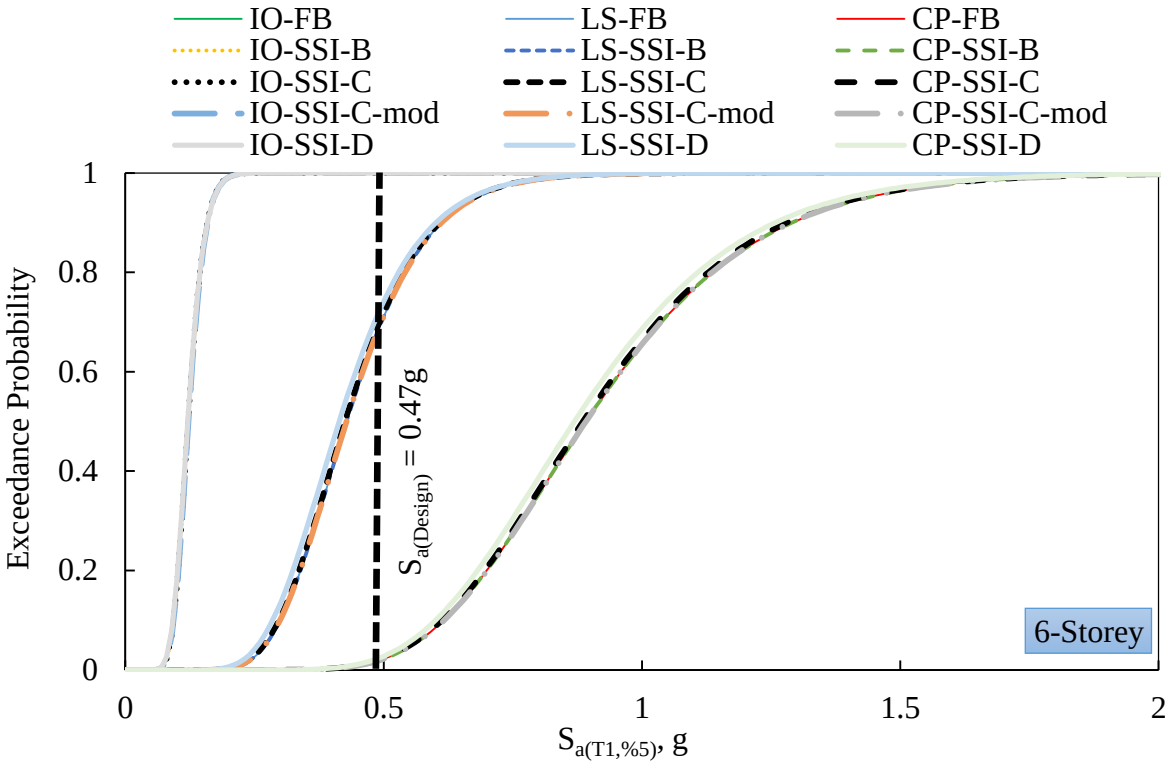
IO-FB
LS-FB
CP-FB
IO-SSI-B
LS-SSI-B
CP-SSI-B
IO-SSI-C
LS-SSI-C
CP-SSI-C
IO-SSI-C-mod
LS-SSI-C-mod
CP-SSI-C-mod
IO-SSI-D
LS-SSI-D
CP-SSI-D
Exceedance Probability
0
0.2
0.4
0.6
0.8
1
0
0.5
1
1.5
2
$S_{a(T1,\%5)}$, g
$S_{a(Design)}$ = 0.47g
6-Storey

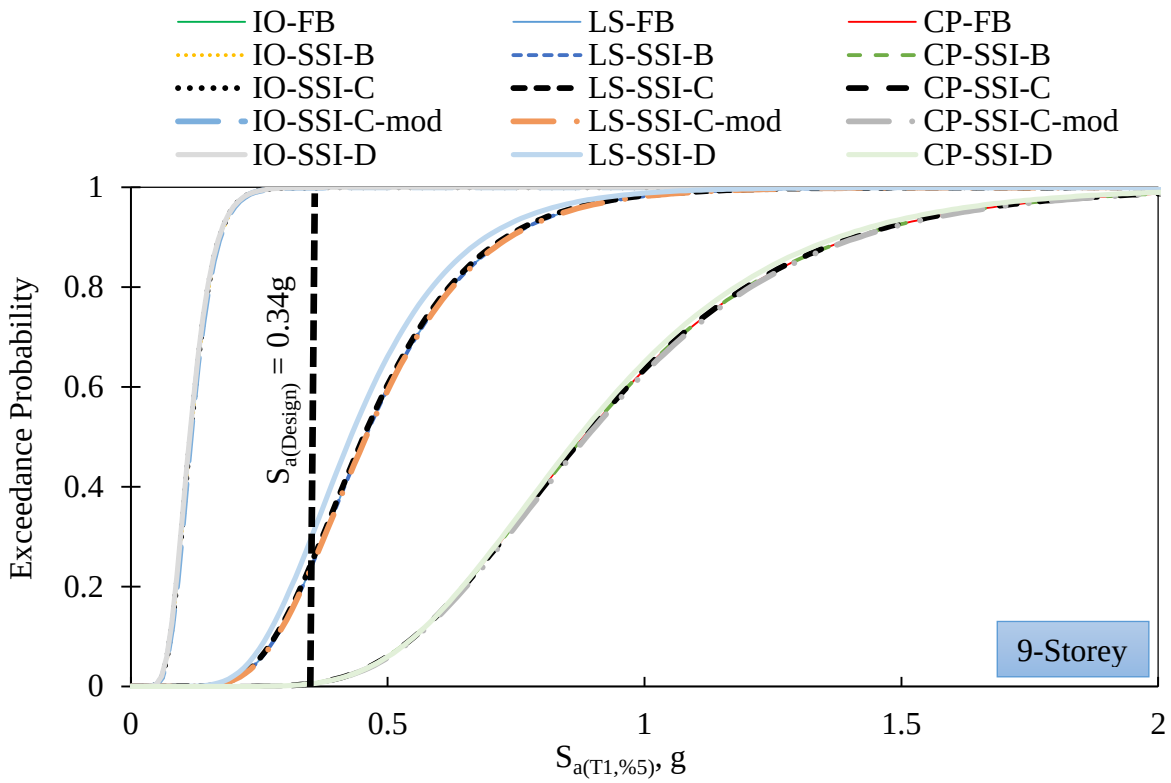
IO-FB
IO-SSI-B
IO-SSI-C
IO-SSI-C-mod
IO-SSI-D
LS-FB
LS-SSI-B
LS-SSI-C
LS-SSI-C-mod
LS-SSI-D
CP-FB
CP-SSI-B
CP-SSI-C
CP-SSI-C-mod
CP-SSI-D
Exceedance Probability
1
0.8
0.6
0.4
0.2
0
0
0.5
1
1.5
2
Sa(Design) = 0.34g
Sa(T1,%5), g
9-Storey

Figure 9.

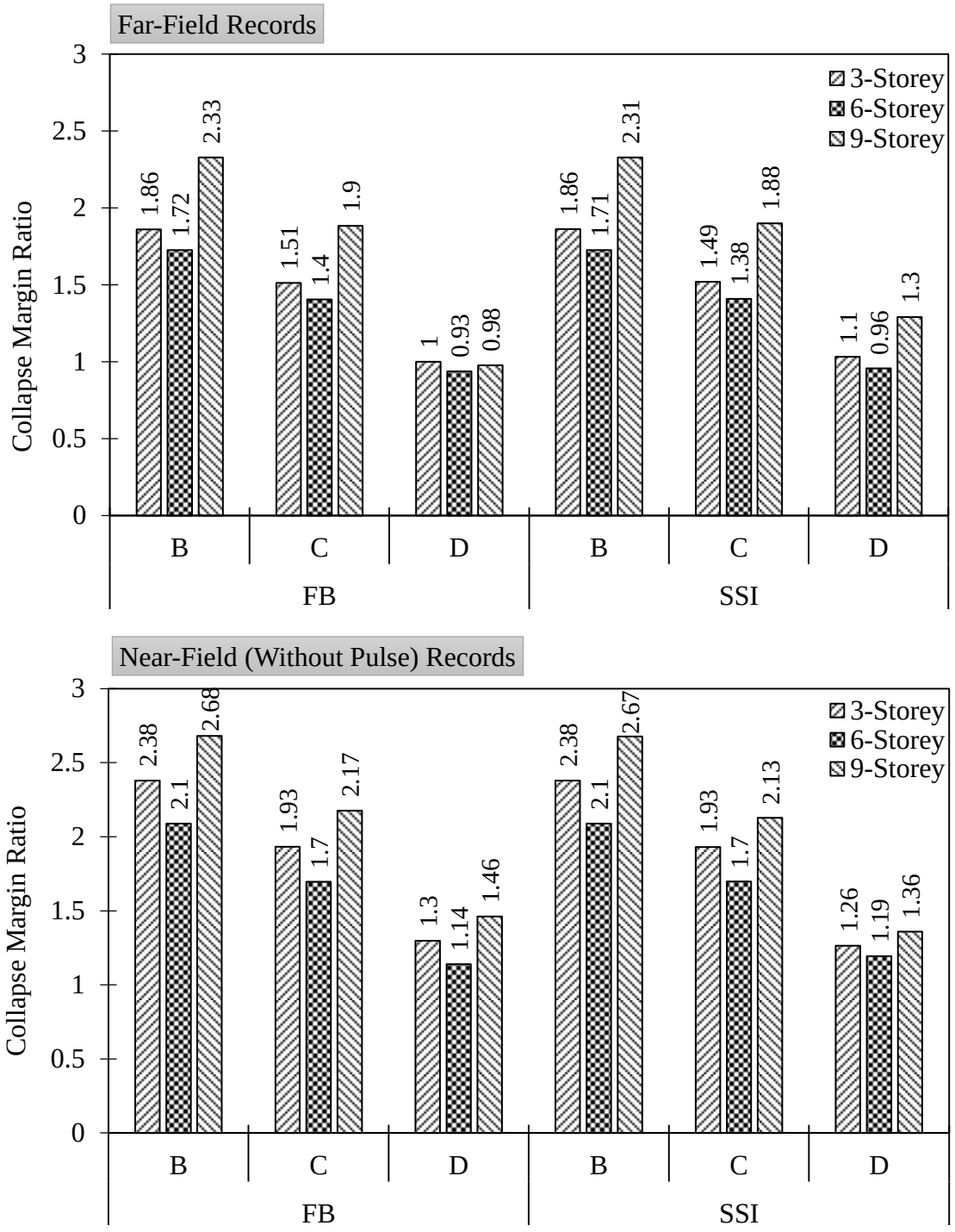
Far-Field Records
Collapse Margin Ratio
3-Storey
6-Storey
9-Storey
1.86
1.72
2.33
1.51
1.4
1.9
1
0.93
0.98
1.86
1.71
2.31
1.49
1.38
1.88
1.1
0.96
1.3
B
C
D
B
C
D
FB
SSI
Near-Field (Without Pulse) Records
Collapse Margin Ratio
3-Storey
6-Storey
9-Storey
2.38
2.1
2.68
1.93
1.7
2.17
1.3
1.14
1.46
2.38
2.1
2.67
1.93
1.7
2.13
1.26
1.19
1.36
B
C
D
B
C
D
FB
SSI

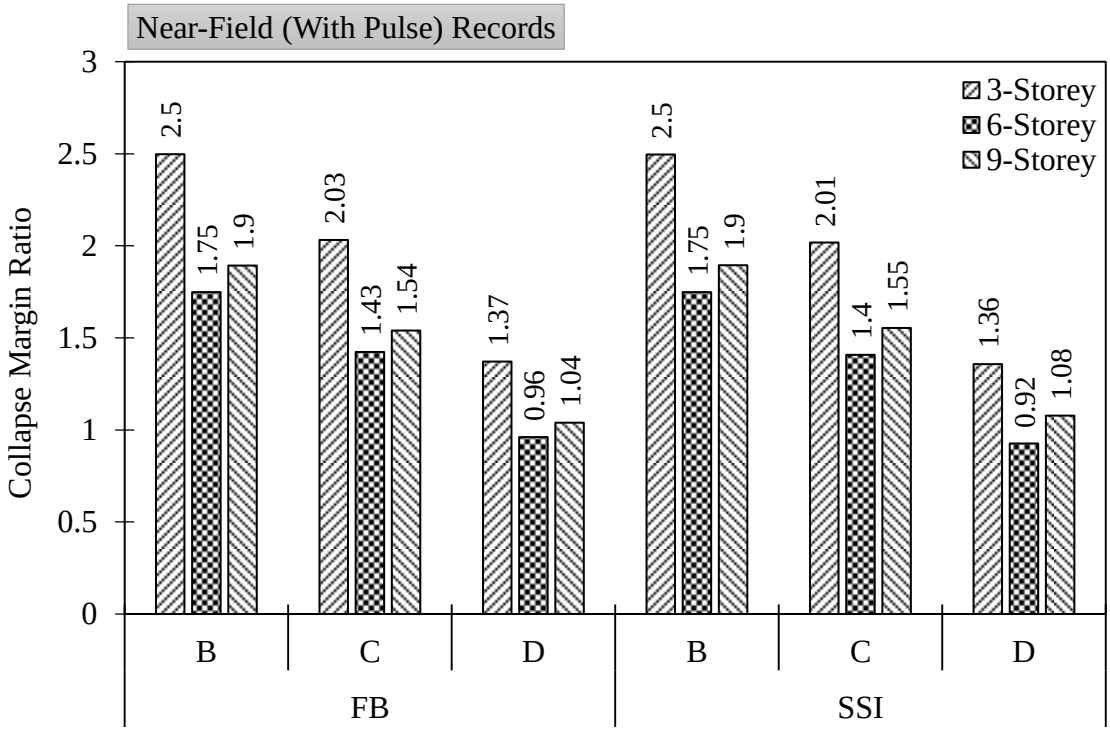
Near-Field (With Pulse) Records
Collapse Margin Ratio
3
2.5
2
1.5
1
0.5
0
3-Storey
6-Storey
9-Storey
2.5
1.75
1.9
2.03
1.43
1.54
1.37
0.96
1.04
2.5
1.75
1.9
2.01
1.4
1.55
1.36
0.92
1.08
B
C
D
B
C
D
FB
SSI

Fig. 10.